Chemistry Africa
https://doi.org/10.1007/s42250-023-00697-1

ORIGINAL ARTICLE

Comparative Study on Structural, Mechanical, Optical and Dielectric Properties of L-Alanine Cadmium Chloride and Manganese L-Alanine Cadmium Chloride Crystal

T. Retna Kumar[1] · M. Abila Jeba Queen[2] · K. C. Bright[3] · R. Ilangovan[4] · K. Sankaranarayanan[5]

Received: 8 February 2023 / Accepted: 3 May 2023
© The Tunisian Chemical Society and Springer Nature Switzerland AG 2023

Abstract
Here in, we reported the comparative study of L-Alanine Cadmium chloride (ACC) and Manganese L-Alanine Cadmium chloride (MnACC) crystal on its growth, structural, mechanical, optical and dielectric properties for NLO applications. Initially ACC and MnACC single crystals were grown at the ambient temperature by solvent evaporation solution growth technique. Both crystals are members of the monoclinic crystal system, according to an X-Ray Diffraction investigation. The crystals were identified as belonging to the soft material category by Vickers micro hardness investigations, which also measured the crystal's yield strength and tensile strength. Optical studies exhibit lower cut off wavelength and the linear and non linear transmittance enhances in the visible region. Dielectric natures of the samples were studies and the activation energy at 100 Hz was found to be as 0.16 eV and 0.26 eV for L-Alanine Cadmium chloride (ACC) and Manganese L-Alanine Cadmium chloride respectively. The effects of manganese on the functional groups are analyzed using Fourier Transform Infra Red (FTIR) analysis.

Keywords Yield strength · Ultimate tensile stress · L-alanine cadmium chloride · Activation energy

1 Introduction

Information technology and industrial applications are significantly impacted by Non Linear Optical (NLO) materials, which play a significant role in the field of nonlinear optics. But over the past decades, there has been a significant improvement in our knowledge of the nonlinear polarization mechanisms and its structural properties. This evolution has been greatly aided by the recent discovery of technology for the manufacturing and growth of optical materials [1, 2]. A metal with modest activity and too brittle is manganese, it provides benefits such as adding stiffness, hardness and strength to the binding metals. The addition of manganese with the metal complex makes the materials well resistant to rusting, mechanical shock and corrosion. About 1% of manganese is included in steel, which improves workability, wear resistance and strength. In addition to being a rubber additive and an oxidizing agent, manganese oxide is also used to make ceramics, glass, fertilizers and ceramics [3]. High optical nonlinearity can be seen in semi organic NLO crystals made of inorganic materials and amino acids. Individually, majority of the amino acids experiences NLO characteristic. An amino group, a carboxyl group, a hydrogen atom, and a characteristic R group (side chain) are all bound to a carbon to form an amino acid. Amino acid shows optical activity from this tetrahedral arrangement of four distinct groups centered on carbon. At neutral pH, amino acids primarily exist as dipolar ions (or zwitterions) rather than un-ionized molecules in solution. When an amino acid is in dipolar state, the carboxyl group is dissociated and the amino group is protonated. Alanine is the

✉ M. Abila Jeba Queen
jeba.abi@gmail.com

1 Department of Nanoscience and Nanotechnology, Alagappa University, Karaikudi 630003, India

2 Department of Physics, Holy Cross College (Autonomous), Nagercoil 629004, India

3 Department of Physics, Mar Ivanio's College (Autonomous), Thiruvananthapuram, Kerala 695015, India

4 National Centre for Nanoscience and Nanotechnology, Guindy Campus, University of Madras, Chennai 600025, India

5 Department of Physics, Alagappa University, Karaikudi 630003, India

Published online: 13 May 2023

simplest amino acid, which just has a methyl group as a side chain [4, 5].

The team Kathleen et al. [6] condensed the pure compound, namely (ACC) first and the team Dhanuskodi et al. [7] subsequently reported the crystals optical phenomena. Likewise, Kalaiselvi et al. [8] reported the parent compound's optical response. The injection of the impurities has impacted the parent compound's characteristics widely. When potassium is doped with the principal compound described by K.C. Bright et al. [9], the dielectric characteristics are improved. By including impurities like cobalt and nickel, the magnetic characteristics of the primary compounds are altered [10, 11]. When copper is added to the L-Alanine cadmium chloride lattice, the linear optical characteristics increase [12]. Trying to improve the physical properties of the host materials, manganese a hard metal but easily oxidized was incorporated as dopants with the ACC. Small addition of manganese is used to deoxidize the metal alloy and enhances its mechanical properties. As notable research has not made on the fabrication and characterization of manganese added L-Alanine Cadmium chloride crystals (MnACC), the present work elucidated the growth of MnACC crystal using simple solvent evaporation technique and their structural properties are analyzed with the aid of single crystal and powder X-Ray Diffraction. Furthermore the grown MnACC materials mechanical (micro hardness), linear (UV–Vis–NIR), non linear optical (SHG), dielectric properties were compared with the ACC crystal.

2 Experimental Methods

L-Alanine and Cadmium chloride were combined in an equimolar ratio to create ACC, which then underwent the following reaction to generate adduct:

$$CH_3CHNH_2COOH + CdCl_2 \rightarrow CH_3CHNH_2COOH \cdot CdCl_2$$

To generate a homogenous mixture, the calculated amounts of the reactants were thoroughly dissolved in double-distilled water and vigorously agitated for about two hours. In order to avoid probable breakdown, the mixture was then heated below its optimal temperature of 333 K and evaporated to dryness. After that, it was completely dissolved in twice-distilled water to create a saturated solution. The solution was thoroughly filtered to remove any suspended contaminants before being allowed to crystallize naturally at room temperature (303 K) for around four weeks with a pH of 5.0. In four weeks, well-defined single crystals with high transparency of $6 \times 5 \times 4$ mm^3 were formed.

To generate MnACC crystal, a homogenous mixture was formed by the combination of reactants such as L-Alanine, Cadmium chloride and Manganese chloride and solvent distilled water. The calculated equal molar quantities of reactants L-Alanine, cadmium chloride and one molar percentage of manganese chloride as a dopants were thoroughly dissolved in double-distilled water and vigorously agitated for about two hours. In order to avoid probable breakdown, the mixture was then heated below its optimal temperature of 333 K and evaporated to dryness. After that, it was completely dissolved in twice-distilled water to create a saturated solution. The solution was thoroughly filtered to remove any suspended contaminants before being allowed to crystallize naturally at room temperature (303 K) for around four weeks with a pH of 5.0. In three weeks, well-defined single crystals with high transparency of $9 \times 6 \times 4$ mm^3 were formed shown in Fig. 1.

3 Result and Discussion

3.1 Structural Analysis

Phase investigation of the crystalline planes was done using Philips X'pert Pro powder X-ray Diffractometer. The X-ray scanning's were made using CuKα radiation with the applied tube voltage of 40 kV and tube current 30 mA. The phase identification was performed using X'pert High score software with the ICDD-PDF-2 data base and all the diffracted peaks were indexed as shown in Fig. 2. The sharp peaks

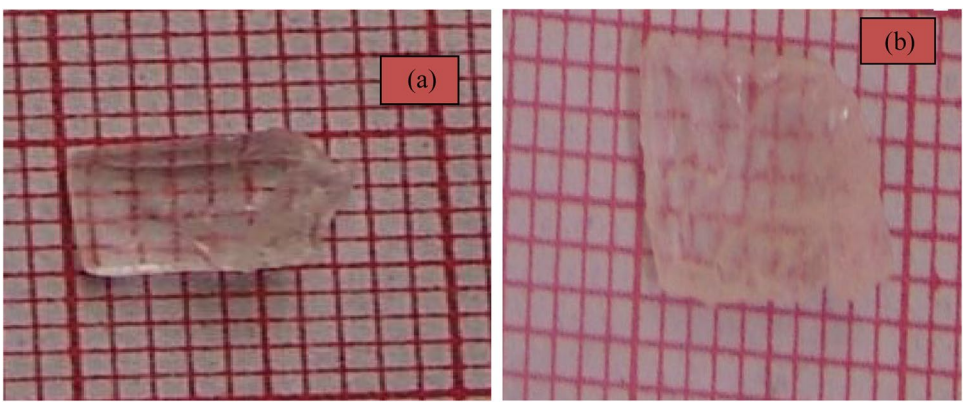

Fig. 1 Grown crystals **a** ACC, **b** MnACC

confirm the crystalline nature, single phase and purity of the grown crystals.

The structural property of the crystals were fetched using a computer controlled Enraf Nonius–CAD4 single crystal diffractometer with Mo-Kα radiation of wavelength 0.71073 Å. The computed unit cell parameter reveals that both the crystal belongs to monoclinic crystal system and the detailed unit cell parameters are depicted in Table 1. Furthermore the manganese concentration in the crystal was estimated with the aid of Atomic Absorption Spectroscopy (AAS). The study affirms that the concentration of Mn^{2+} ions inculcated in the ACC crystals is 227 ppm. Thus the structural analysis using X-rays witness that the manganese chloride has not made any changes in the crystal system but shows slight variations in lattice parameters.

Table 1 Unit cell parameters

Parameters	ACC	MnACC
a (Å)	16.33	16.29
b (Å)	7.31	7.27
c (Å)	8.00	7.98
α, β, γ	α = γ = 90°, β = 116.44°	α = γ = 90°, β = 116.49°
Cell volume(Å$^{3)}$	854	845.83
Space group	C_2	C_2
Effective number of atoms	4	4

3.2 Mechanical Studies

In order to analyze the effect of manganese on the mechanical properties of the crystal, micro hardness studies of ACC and MnACC crystals were performed out by admitting the crystal into Leitz micro hardness tester with the applied load from 0.025 to 0.100 kg on the selected (101) plane. The micro hardness number (H_v) was calculated [13] by applying the load (P) and the average diagonal length (d) using the relation (1) and the plot is shown in Fig. 3.

$$\mathrm{Hv} = \frac{1.8544\ \mathrm{P}}{d^2}\ \mathrm{kg\ mm^{-2}}. \quad (1)$$

The plot of Vickers's micro hardness number and applied load elucidates that, as the applied load increases the micro hardness number also increases in both crystals. Again for MnACC crystals, the micro hardness number is found to be greater than that of ACC crystal due the effect of manganese into well defined lattice of ACC. Thus the addition of manganese improves the micro hardness of the parent compound.

Using the Mayer's formula, the relation between load (P) and the diagonal length (d) of the crystal was studied and the work hardening coefficient (n) is obtained from the slope of log d vs. log P. The Mayer's formula is:

$$\mathrm{P} = \mathrm{kd^n} \quad (2)$$

The slope of the straight line in Fig. 4 gives work hardening coefficient values 3.5466 and 3.5945 for ACC and MnACC crystals are respectively. According to Onitsch [14] and Hanneman, if n lies between 1–1.6 the materials belongs to the category of soft material [15]. Hence the micro hardness test witnessed that both the crystals belong to the category of soft material. Using the experimental data, the other mechanical parameters such as yield strength, ultimate tensile strength and elastic stiffness constant values calculated are shown in Table 2.

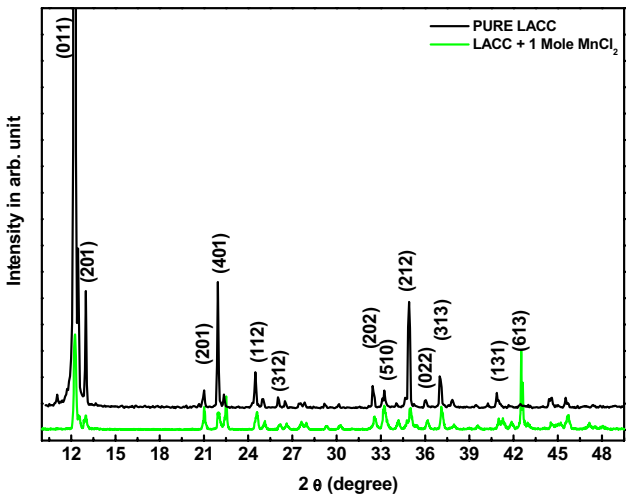

Fig. 2 Powder XRD pattern

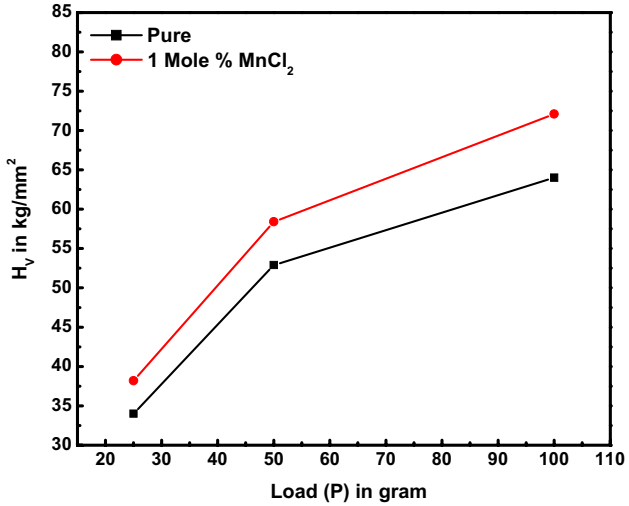

Fig. 3 Variation of micro hardness number with applied loads

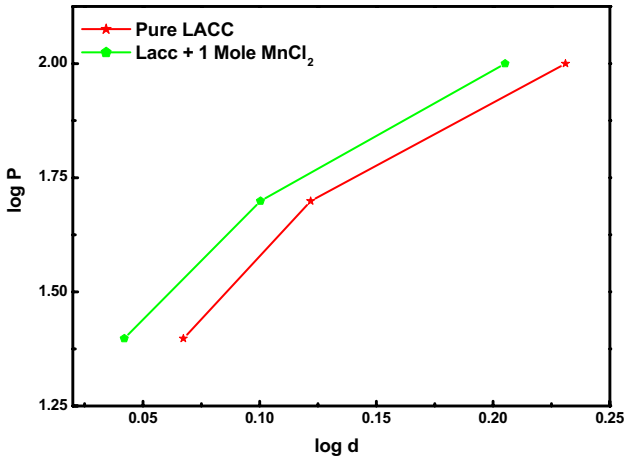

Fig. 4 log d vs. log P plot

Table 2 Mechanical properties

Parameters	ACC	MnACC
Vickers's micro hardness number (Kg/mm^2)	48.33	56.17
Work hardening coefficient	3.5466	3.5945
Yield strength (GN/m^2)	43	39
Ultimate tensile strength (MPa)	434	552
Elastic stiffness constant (10^{14} Pa)	88.6	115.2

Yield strength (σ_y) of the crystal determines the point at which the material undergoes plastic deformation. Using Hollomon's equation [16], the elastic limit of the material can be calculated using the relation

$$\sigma_y = H_v(0.002)^n \quad (3)$$

Ultimate tensile strength (σ_u) of the crystal is the maximum load applied to the crystal can withstand before rupture.

$$\sigma_u = H_v\, n^n \quad (4)$$

Elastic stiffness constant (C_{11}) of the material was evaluated from the Wooster's empirical formula [17] and gives the information about the stiffness between the atoms.

$$C_{11} = \left(H_v\right)^{1.75} \quad (5)$$

When manganese is added to the ACC crystal, its mechanical parameters such as micro hardness, work hardening coefficient, ultimate tensile strength and elastic stiffness constant increases slightly meanwhile the yield strength value decreases. Yield strength in the crystal determines the stress level that indicates dislocation motion between the crystalline planes. Therefore manganese boosts the mechanical properties and reduces the dislocation motion between the crystalline planes.

3.3 Optical Studies

The UV–Vis–NIR spectrum was recorded using UV–Vis spectrophotometer in the wavelength range 200–2500 nm and is depicted in Fig. 5.

The absorbance spectrum confirms that the addition of manganese ions decreases the absorbance percentage of the grown crystals due to the fact that manganese ions are easily oxidized when combines with ACC. Thus it improves the transparency of the MnACC crystals. The crystal experiences lower cutoff wavelength of 220 and 240 nm for ACC and MnACC respectively near the UV region and exhibits absorption in the range of blue light. This is mainly due to the transitions of $p \rightarrow p^*$ and charge transfer between metal–organic ligands. The lower cutoff wavelength

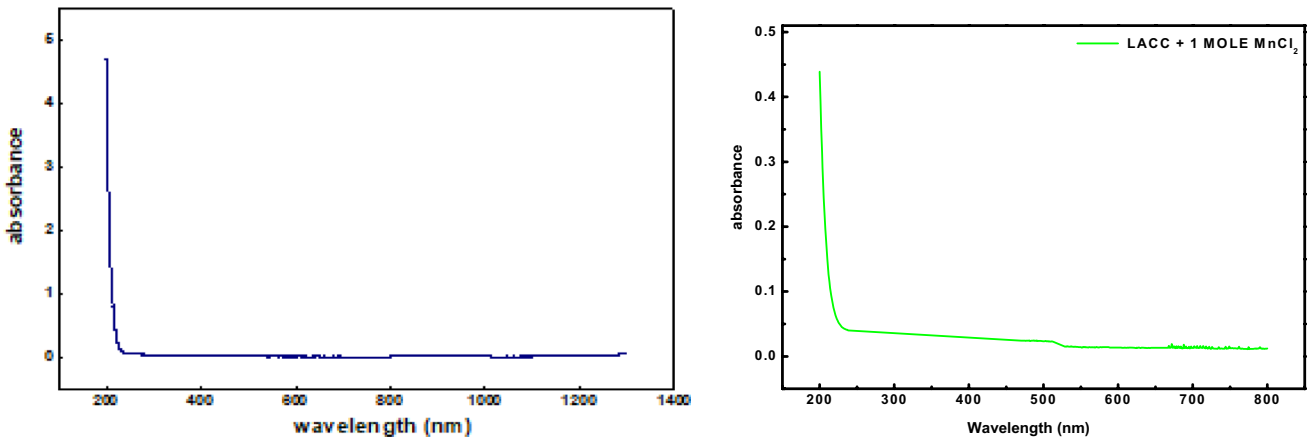

Fig. 5 UV–Visible absorbance spectrum

(200–400 nm) is the necessary condition of the crystal capable for blue light by second harmonic generation from diode laser [18, 19]. Furthermore blue shift in the lower cut off wavelength around 240 nm experiences due to the electronic transition between carboxylate and nitrate bonds [20]. Due to the lower electron affinity of manganese, the material is which is considered as a required phenomenon of NLO properties.

The SHG measurements of the grown crystals were performed using the Kurtz and Perry powder technique. The input LASER energy source is allowed to incident on the capillary tube 4.3 mJ/5.3 mJ per pulse in order to optimize energy level to eliminate chemical decomposition. The SHG efficiency of ACC and MnACC crystals was 0.57 and 0.88 times of KDP. The SHG efficiency of ACC is very much changed by the manganese and best performance is obtained for elements with smaller ionic radii (0.8A) compared to cadmium (0.96 A). This is due to the change in polarizability of the manganese ions present and hence the materials can be used as an efficient frequency conversion material.

3.4 Dielectric Studies

Capacitance and dielectric loss measurements were carried out using Agilent 4284 A, Precision model LCR meter in the frequency range of 100 Hz–1 MHz at the temperature range of 30–110 °C. The grown crystals were cut, polished and graphite coated for better electrical contact of the material.

From the plot (Fig. 6), it was observed that the dielectric constant of ACC and MnACC crystals decreases with increase of frequency. The peak value of dielectric constant observed at lower frequency, which happens mainly due to the contribution of all types of polarization namely electronic, ionic, oriental and space charge polarization [12]. Because of its higher space charge polarization in the low frequency region the maximum value of dielectric constant experienced after the application of frequency space charge polarization cannot withstand therefore the polarization decreases [21].

When an a.c voltage was applied to the prepared sample, fraction of the electrical energy absorbed and the remaining dissipated in the form of heat energy, the corresponding energy loss is called dielectric loss. When it comes to heat generation and high voltage applications, the dielectric loss was considered to be a highly crucial parameter. The dielectric loss as a function of frequency for pure and Mn^{2+} ions doped ACC crystals are given in the following Fig. 7.

The variations in dielectric loss with frequency indicate that the loss gets smaller as the frequency rises. As a result of materials with fewer dipoles per unit volume than a material with a greater dielectric constant, the material with a low dielectric constant will have the lowest loss. At higher frequencies, the value of dielectric loss reduces. Manganese

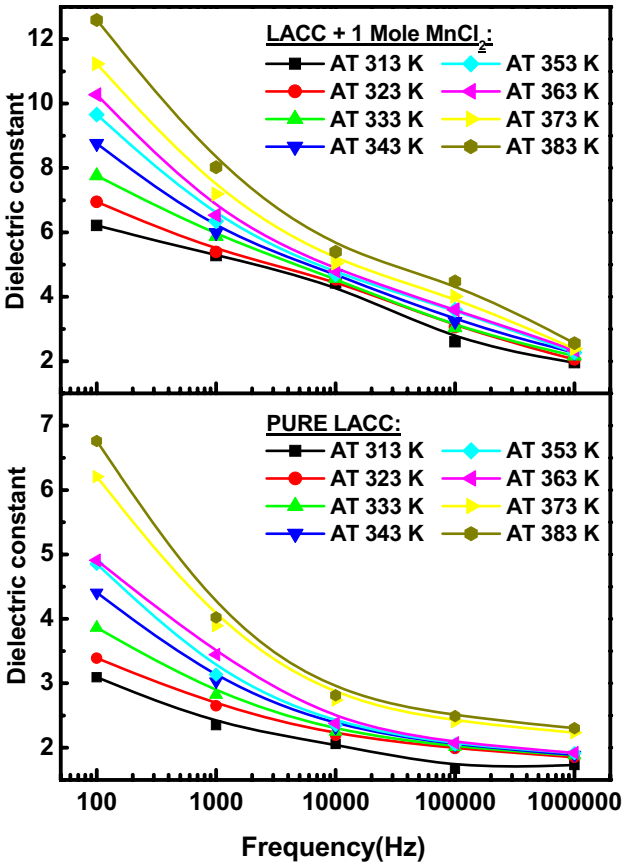

Fig. 6 Variation of dielectric constant at frequencies

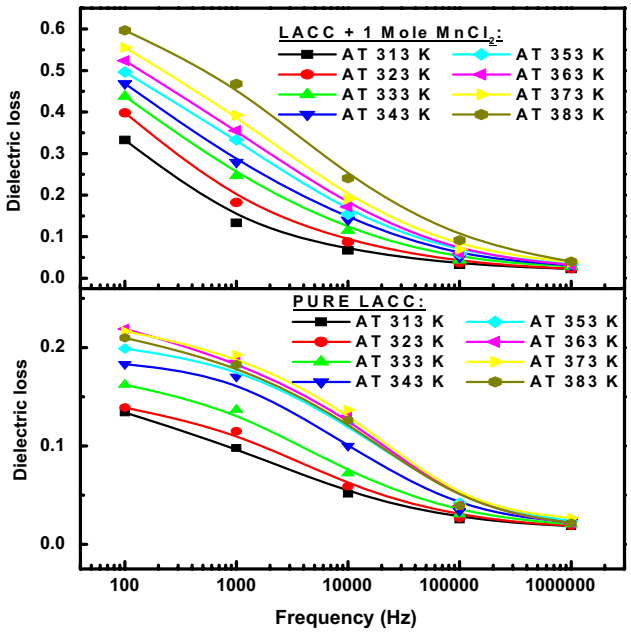

Fig. 7 Dielectric loss with frequencies at different temperature

doping increases dielectric constant and decreases dielectric loss. Thus the crystal should be satisfactory to possible application in microelectronics [22]. The crystals NLO application owing to the low value of dielectric loss at higher frequencies, which again indicates that the crystal has improved optical quality with fewer defects.

Measurement of AC conductivity provides precise information regarding localized charges. The crystal's dislocations give rise to the localized electronic states that are present there. The dielectric constant and dielectric loss values of ACC and MnACC are used to compute the AC conductivity shown in Figs. 8 and 9. The slope of the 1000/T and ln σ_{ac} curve gives the value of E_{ac}/K_B and hence the activation energy of pure and Mn doped ACC is 0.16 eV and 0.2551 eV at 100 Hz and 0.1247 eV and 0.2084 eV at 1000 Hz.

It was evident that when the frequency of applied ac voltage is low, more energy is required to activate the atoms or molecules, whereas when the frequency is higher, less energy is required for the same system to activate the atoms or molecules. The value of ac activation energy at frequency 100 Hz is greater than that at frequency 1000 kHz. Additionally; MnACC crystals have higher activation energies than the ACC crystals. This demonstrates how crystal defects or impurities will raise the activation energy of doped crystals.

3.5 Functional Group Identification

The FTIR spectra of ACC and MnACC crystals were analyzed in the range of 400–4000 cm^{-1} following KBr pellet technique and the corresponding FTIR spectra's are given in Figs. 10 and 11.

The broad envelope in the higher energy region 3044–3250 and 3425–3500 cm^{-1} in ACC and 3076–3228

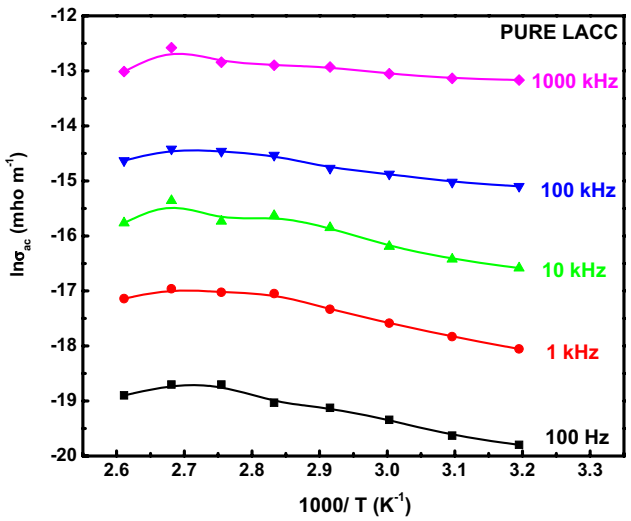

Fig. 8 The 1000/T vs. ln σ_{dc} plot for ACC crystal

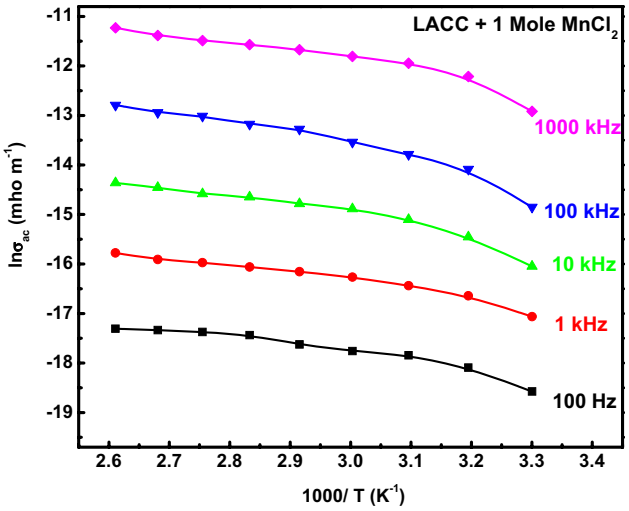

Fig. 9 The 1000/T vs. ln σ_{dc} plot for MnACC

and 3400–3525 in MnACC is due to NH^{3+} symmetric and antisymmetric stretching vibrations. The absorption peak at 1616 cm^{-1} in ACC and 1595 cm^{-1} in MnACC is assigned to NH^{3+} bending degenerate mode [23]. The region of absorption bands from 3044 to about 2500 cm^{-1} in ACC, 3076–2599 cm^{-1} in MnACC is due to multiple combinations of overtone bands. The strong absorption peak at 1412 cm^{-1} in ACC and 1417 cm^{-1} in MnACC corresponds to COO^- symmetric stretch [24]. The COO^- bending and rocking frequencies occur in the normal positions at 762, 622 and 536 cm^{-1} in ACC and for Mn doped ACC which is at 766, 631 and 544 cm^{-1}. Also the absorption at 1343 and 1001 cm^{-1} in ACC, 1347 and 1012 cm^{-1} in Mn doped ACC are due to CH_3 symmetric bending and rocking mode. The absorption peaks at 923 and 841 cm^{-1} in pure, 923 and 848 cm^{-1} in MnACC are assigned to C–C–N symmetric stretching vibrations. These vibrations prove that the presence of expected functional groups in the compound. It is observed that there are slight shifts, broadening and narrowing of absorption peaks in FTIR spectrum Manganese doped ACC crystals and this may be due to the incorporation of dopant ions into the crystal lattice.

4 Conclusion

Good quality single crystals namely, Here L-Alanine Cadmium chloride (ACC) and Manganese L-Alanine Cadmium chloride (MnACC) single crystal was successfully grown by solvent evaporation crystal growth technique. X-Ray Diffraction studies reveal that the synthesized crystals appear under the monoclinic crystal system. Increasing hardness with the application of the load exhibits the

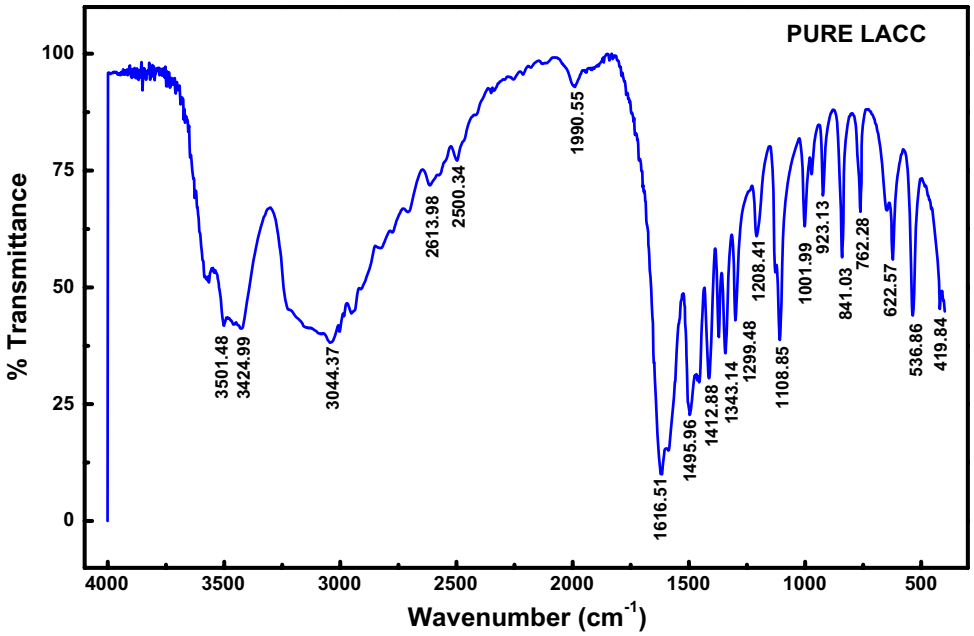

Fig. 10 FTIR spectrum of ACC

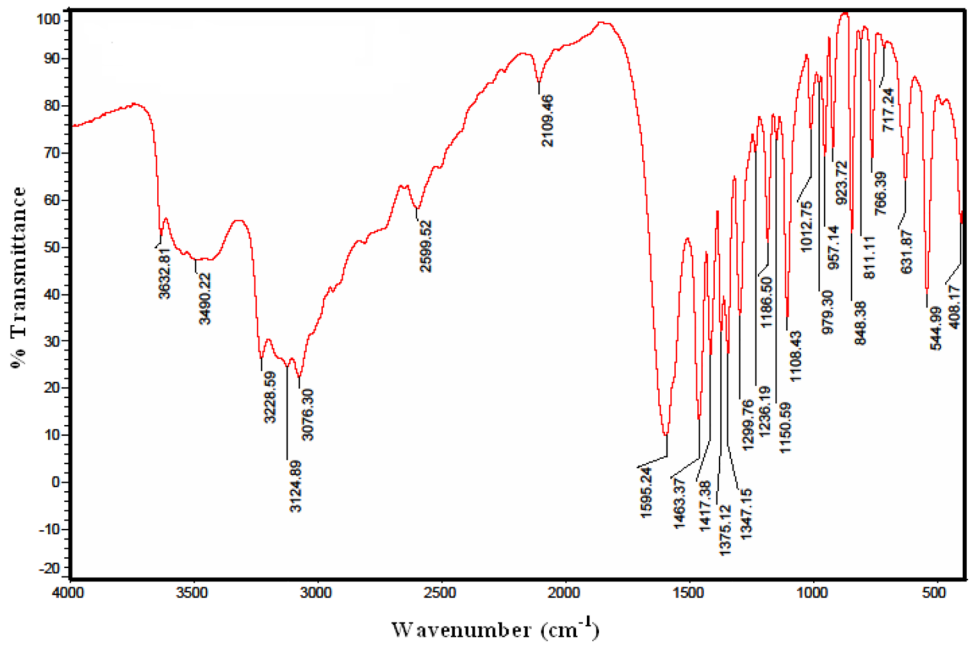

Fig. 11 FTIR spectrum of MnACC

material as a soft category with high tensile strength. Compared to ACC, MnACC shows high transparency and NLO response. Dielectric constant and loss decreases with respect to the applied frequency. Activation energy was found to be increasing due to the addition of manganese. Due to the addition of manganese, the FTIR spectrum shows slight shift, broadening and narrowing of absorption peaks. Thus the crystals with good tensile, optical and dielectric properties are identified as a potential candidate for Liquid Crystal Displays.

Author Contributions All authors contributed equally to the study, conception, design and all the authors commented on the previous versions of the manuscript. All authors read and approved the final manuscript.

Data Availability The datasets generated during and/or analysed during the current study are available from the corresponding author on reasonable request.

Declarations

Conflict of interest The authors declare that they have no known competing financial interests or personal relationships that could have appeared to influence the work reported in this paper.

Ethical Approval This article does not contain any studies involving human participants or animals performed by any of the authors.

References

1. Arivuoli D (2001) J Phys 57:5
2. Pricilla Jeyakumari A, Ramajothi J, Dhanuskodi S (2004) J Cryst Growth 269:558
3. F. Holleman Arnold, W Egon, W Nils, M Lehrbuch der, An. Organis. Chen. Chemie", pp. 1110-1117
4. Stryer L (1995) Biochemistry, 4th edn. W H Freeman and Company, New York
5. Ushasree PM, Muralidharan R, Jayavel R, Ramasamy P (2000) J Cryst Growth 218:365
6. Kathleen Schaffers I, Doughlas Keszler A (1993) Acta Cryst C 49:1156
7. Danushkodi S, Vasantha K, Angeli Mary PA (2007) Spectro Chim Acta Part A 66:637
8. Kalaiselvi P, Alfred Cecil Raj S, Vijayan N (2013) Optik 124:6978
9. Bright KC, Freeda TH (2010) Phys B 405:3857
10. Benila BS, Bright KC, Mary Delphine S, Shabu R (2017) J Magn Mater 426:390
11. Benila BS, Bright KC, Mary Delphine S, Shabu R (2018) Opt Quant Electron 50:202
12. Benila BS, Bright KC, Mary-Delphine S, Abila-Jeba-Queen M, Shabu R (2018) J Appl Sci Comput 5:626
13. Sangwal K, Surovska B (2003) Mater Res Innov 7:91
14. Onitsch EM (1956) Mikroskopie 95:12
15. Mott BW (1956) Micro indentation hardness testing. Butterworths, London
16. Hollomon JH (1945) Tensile deformation. Trans AIME 162:268
17. Wooster WA (1953) Rep Prog Phys 16:62
18. Abila Jeba Queen M, Bright KC, Mary Delphine S, Aji Udhaya P (2021) J Mater Sci Mater Electron 32:13261
19. Le Fur Y, Masse R, Cherkaoui MZ, Nicoud JF (1995) Cryst Mater 210:856
20. Abila Jeba Queen M, Bright KC, Mary Delphine S, Aji Udhaya P (2019) Spectrochim. Acta A 228:117802
21. Abila Jeba Queen M, Bright KC, Aji Udhaya P (2023) J Mater Sci: Mater Electron 34:181
22. Liu H, Xiong Y, Chen S, Yang C, Bian J, Feng Y, Fang B, Gao X (2022) J Alloys Compd 891:162098
23. Nagamoto K (1978) IR and Raman Spectra of inorganic and coordination compounds. John Wiley and Sons, New York
24. Silverstein R, Bassler GC, Morril TC (1981) Spectrometric identification of organic compounds. John Wiley & Sons, Newyork

Springer Nature or its licensor (e.g. a society or other partner) holds exclusive rights to this article under a publishing agreement with the author(s) or other rightsholder(s); author self-archiving of the accepted manuscript version of this article is solely governed by the terms of such publishing agreement and applicable law.